

# Fixing multiple waveguides induced by photorefractive solitons: directional couplers and beam splitters

Aqiang Guo, Michael Henry, and Gregory J. Salamo

*Department of Physics, University of Arkansas, Fayetteville, Arkansas 72701*

Mordechai Segev

*Department of Physics, Technion-Israel Institute of Technology, Haifa 32000, Israel, and  
Department of Electrical Engineering, Princeton University, Princeton, New Jersey 08544*

Gary L. Wood

*U.S. Army Research Laboratory, AMSRL-SE-EO, Adelphi, Maryland 20783-1197*

Received April 11, 2001

We show how to transform multiple real-time photorefractive solitons into permanent two-dimensional single-mode waveguides impressed into the crystalline lattice of the host material. We experimentally demonstrate two specific configurations of such fixed multiple waveguides: directional couplers and multiple beam splitters. © 2001 Optical Society of America  
OCIS codes: 190.5530, 190.5330.

Photorefractive solitons<sup>1</sup> have been observed at low light powers and exhibit robust trapping in both transverse dimensions.<sup>2–6</sup> Among the numerous types of photorefractive soliton, the most commonly used type is screening solitons,<sup>7–10</sup> which form when an electric field applied to a photorefractive crystal is partially screened within the incident light beam as a result of transport of photoexcited charges. As a result, an internal electric field exists around the optical beam and modifies the refractive index through the Pockels effect. The parameters of soliton self-induced waveguides can be engineered by use of the soliton existence curve.<sup>11</sup> Such soliton-induced waveguides can be used in various waveguide applications and in multiple configurations, such as directional couplers<sup>12</sup> and beam splitters (Y junctions),<sup>13–15</sup> (as was demonstrated with other kinds of solitons),<sup>16</sup> and more recently were used to obtain a waveguiding environment for efficient nonlinear frequency conversion.<sup>17,18</sup> However, these real-time waveguides induced by photorefractive solitons decay and disappear when the applied field is turned off while the waveguides are guiding a light beam. This decay and disappearance occur because the trapped electrons that have screened the applied electric field are re-excited and undergo transport, giving rise to a charge distribution that cannot support solitons. Although the self-induced and easily erased nature of photorefractive soliton-induced waveguides is attractive for dynamic applications, for many applications it is advantageous to impress waveguides into the crystalline structure permanently, that is, to have the induced waveguide last indefinitely without an applied field, even under intense illumination. Recently, Klotz *et al.*<sup>19</sup> and DelRe *et al.*<sup>20</sup> demonstrated how to transform the “real-time” screening soliton into a permanent waveguide by means of ferroelectric domain reversal.<sup>19,20</sup> Here, we experimentally demonstrate the fixing of multiple photorefractive solitons into permanent two-dimensional single-mode

waveguides that also act as directional couplers and multiple beam splitters.

We start by demonstrating the process of fixing two soliton-induced waveguides into a directional coupler. A directional coupler consists of two waveguides in close proximity, which are coupled to each other by evanescent fields. The separation between the waveguides determines the coupling efficiency. The closer the waveguides are to each other, the larger the coupling is. In principle, in a directional coupler consisting of two completely identical waveguides, as much as 100% of the energy injected into one waveguide can be transferred into the second waveguide after a specific propagation distance  $L$ . For lengths less than  $L$  the coupling is less than 100%, whereas for lengths greater than  $L$ , energy is coupled back into the original waveguide and the coupling is also less than 100%. A directional coupler made by using real-time soliton-induced waveguides was demonstrated in Ref. 12. In this Letter we generate such a directional coupler and the convert it into a permanent structure, using the technique for fixing photorefractive solitons demonstrated in Ref. 19.

We use the standard setup for forming and fixing screening solitons,<sup>8,11</sup> combined with the technique for generating a soliton-induced directional coupler.<sup>12</sup> Beam splitters divide the output of a 514.5-nm argon-ion laser into two 20- $\mu$ W soliton beams and a 100-mW background beam. The crystal is a 1-cm cube of SBN:75 doped with 0.02% cerium by weight. The soliton beams each have a 12- $\mu$ m FWHM input diameter [Figs. 1(a)–1(c)], and the 100-mW background beam is expanded to fill the entire crystal. Normally, the incident beams, which propagate along an  $a$  axis, diffract to  $\sim 100$   $\mu$ m at the exit face. When an electric field is applied along the  $c$ -axis, the beams self-trap, as the output beam diameters are reduced to 12  $\mu$ m. Once the beam self-focuses to its initial width of 3 kV/cm, we switch off the laser light and the applied electric field sequentially. After 1 min, the

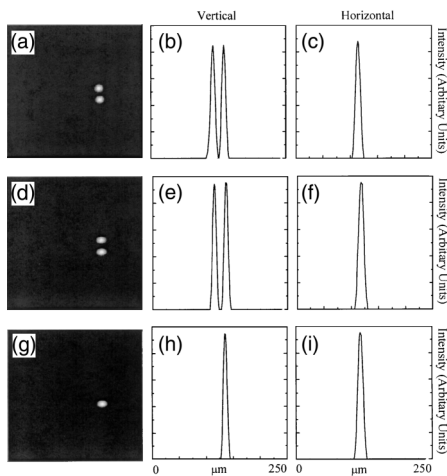


Fig. 1. (a) Photograph both argon input beams on the entrance face and (b) vertical and (c) horizontal input profiles. (d) Photograph of the beams on the exit face with two fixed waveguides and (e) vertical and (f) horizontal exit profiles. (g) Photograph of the exit face with only the upper beam injected and (h) vertical and (i) horizontal exit profiles.

soliton and the background beams are switched back on, but the applied field is held at zero. Experimentally, we first observe the output beam diameter to be  $12\ \mu\text{m}$ , just as before the applied field was set to zero, because the trapped charges are not redistributed in the dark. With the illumination back on, the beam slowly expands to near its original diffracted value, and then, within 2 min, contracts back to the  $12\text{-}\mu\text{m}$  diameter. The two waveguides are now fixed and guide the light with zero applied voltage and no background illumination [Figs. 1(d)–1(f)].<sup>19</sup>

The explanation for fixing, as reported earlier,<sup>11</sup> is that when the solitons form, the field outside the soliton region lowers the index of refraction,  $n_0$ , to a value of  $n_0 - \Delta n$ , where  $\Delta n = r_{\text{eff}} \mathbf{E}_0$ ,  $\mathbf{E}_0$  is the applied field, and  $r_{\text{eff}}$  is the effective electro-optic coefficient. Meanwhile, the index in the soliton region, where the local field is near zero, is a the higher value of  $n_0$ . The transported charge density responsible for the screening results in a negative space-charge field,  $\mathbf{E}_{\text{sc}} \cong -\mathbf{E}_0$ , in the soliton region. When the light and the applied field are switched off, the charge is locked in place. This locking gives rise to a space-charge field of  $\sim -3\ \text{kV/cm}$  within the soliton. At this stage the index profile is  $n_0$  in the region outside the soliton waveguide (where the field is zero) and  $n_0 + \Delta n$  inside the soliton. Therefore, a waveguide is present despite the applied field's being off. In our crystal, the coercive field ( $1\ \text{kV/cm}$ ) is smaller than the amplitude of the space-charge field inside the induced waveguide region, causing domains in this region to flip  $180^\circ$ . Following the reversal of the spontaneous polarization, the space-charge field and the index in the soliton region drop, causing the soliton beam to expand to near its diffracted value. Since the spontaneous polarization is discontinuous at the margins of the soliton, where a domain wall now exists, charges are attracted to this region, making the domain head-to-head structure stable. The final

space-charge field is due to this nonuniform charge distribution and is in the same direction as the original applied field. Inside the soliton region, this field increases the index and forms a waveguide.

After generating a real-time directional coupler<sup>7</sup> and fixing the waveguides to a permanent directional coupler, we measure the coupling between the waveguides, using an 840-nm probe laser beam. At this wavelength, the overlap integral between the modes of the adjacent waveguides is much higher and results in efficient directional coupling. The peak-to-peak separation between the two solitons at the input is 30 and  $32\ \mu\text{m}$  at the output, i.e., almost fully parallel. The intensities and the widths of the two beams are nearly identical, and both solitons are formed with an applied voltage of 400 V. To investigate the coupling between the two soliton fixed waveguides, we launch the probe beam into the lower waveguide [Figs. 2(a)–2(c)] only and observe that a large portion of the energy has coupled from the original waveguide into the other waveguide, as shown in Figs. 2(d)–2(f). The coupling efficiency (the fraction of energy transferred by directional coupling) is  $\sim 33\%$ . For comparison, when only the lower soliton (into which the probe is launched) exists and the crystal is at steady state for a single-soliton input, the probe beam is guided well by the single waveguide [Figs. 2(g)–2(i)]. However, when only the lower soliton is present and the probe beam is still launched into where the upper soliton had been, the probe is not guided but diffracts [Figs. 2(j)–2(l)], and only a tiny part of the probe's energy is trapped by the adjacent

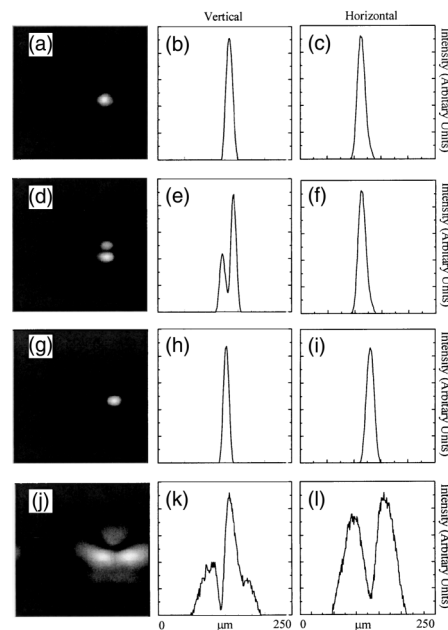


Fig. 2. (a) Photographs of Ti:sapphire input beam on the entrance face injected into the lower waveguide and (b) vertical and (c) horizontal input profiles. (d) Photograph of the beams on the exit face with two fixed waveguides and (e) vertical and (f) horizontal exit profiles. (g) Photograph of the exit face with only the lower beam injected and only the lower waveguide fixed and (h) vertical and (i) horizontal exit profiles. (j) Photograph of the exit face with only the upper beam injected and only the lower waveguide fixed and (k) vertical and (l) horizontal exit profiles.

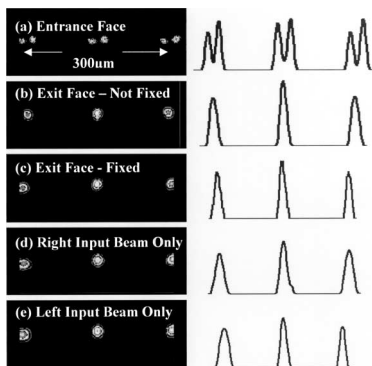


Fig. 3. Three beam splitters (Y junctions) fixed simultaneously. Photographs and profiles of (a) Ti:sapphire input beams on the entrance face, (b) output soliton at the exit face before fixing, (c) output soliton at the exit face after fixing, (d) output soliton at the exit face with only the right input beam, and (e) output soliton at the exit face with only the left input beam.

waveguide. These results show that the coexistence of two fixed soliton waveguides works as a directional coupler and that the probe beam is coupled from one soliton-induced waveguide into the other. We emphasize that the waveguide directional coupler is truly a permanent structure after the fixing process: It survives at room temperature when the applied field is removed even under intense illumination. Nevertheless, applying an electric field that is larger than the coercive field of the crystal can erase the directional coupler. This capability makes possible permanent recording of intricate optical circuitry in the volume of a bulk crystal so that integrated optics need not be limited to a planar geometry.

To demonstrate further the possibility of fixing complex waveguide structures, we investigated the formation of multiple beam splitters. In this case, a diffractive optical element is placed in the path of each soliton argon beam, so that more than one beam splitter (Y junction) could be formed and fixed simultaneously. The diffractive element creates five replicas of the pair of input soliton beams; the replicas are evenly spaced along a line parallel to the  $c$  axis. Each input pair was separated by  $125 \mu\text{m}$ , with peak-to-peak spacing of  $23 \mu\text{m}$  between the  $11\text{-}\mu\text{m}$  members of the pair. Each pair of solitons "fused" and formed a single output soliton. Thus, three output solitons, each with a diameter of  $12 \mu\text{m}$  at an applied field of  $3 \text{ kV}$ , were observed, indicating that three Y junctions were formed (Fig. 3). Each trapped Y junction guided 49% of the total incident power. When the input to one of these Y junctions was blocked, no effect on the other two Y junctions was observed. After fixing, each Y junction maintained independent behavior and had a diameter of  $12 \mu\text{m}$ . With in-phase beams incident on each arm of the Y junction, the fixed output was 49% of the incident energy. With beams incident on each arm, with a relative phase difference of  $\pi$ , no energy was guided by the Y junction. With either the left or the right arm excited, the fixed output was 40% of the incident energy.

In summary, we have shown that two spatial solitons that are propagating nearly parallel and at close proximity can be impressed into a crystalline lattice and serve as directional couplers. The maximum coupling efficiency that we observed was 33% for solitons at  $\lambda = 840 \text{ nm}$  and a propagation length of  $1 \text{ cm}$ . We expect that, for a proper choice of propagation length, the coupling efficiency can be almost unity. In addition, using binary optics to produce multiple input beams at the entrance face of the crystal, we have also demonstrated that sets of beam splitters or Y junctions can be formed. By use of this approach, a linear array of three beam splitters was fixed in the crystal, each of which guided 49% of the incident light.

This work was supported by the U.S. Army Research Office and is part of the Multidisciplinary University Research Initiative program on optical spatial solitons.

## References

1. M. Segev, B. Crosignani, A. Yariv, and B. Fischer, *Phys. Rev. Lett.* **68**, 923 (1992).
2. G. Duree, J. Shultz, G. Salamo, M. Segev, A. Yariv, B. Crosignani, P. DiPorto, E. Sharp, and R. Neurgaonkar, *Phys. Rev. Lett.* **71**, 533 (1993).
3. G. Duree, J. Shultz, G. Salamo, M. Segev, A. Yariv, B. Crosignani, P. DiPorto, E. Sharp, and R. Neurgaonkar, *Phys. Rev. Lett.* **74**, 1978 (1995).
4. M. Segev, G. C. Valley, B. Crosignani, P. DiPorto, and A. Yariv, *Phys. Rev. Lett.* **73**, 3211 (1994).
5. D. N. Christodoulides and M. I. Carvalho, *J. Opt. Soc. Am. B* **12**, 1628 (1995).
6. M. Segev, M. Shih, and G. C. Valley, *J. Opt. Soc. Am.* **13**, 706 (1996).
7. M. D. Iturbe-Castillo, P. A. Marquez-Aguilar, J. J. Sanchez-Mondragon, S. Stepanov, and V. Vysloukh, *Appl. Phys. Lett.* **64**, 408 (1994).
8. M. Shih, M. Segev, G. C. Valley, G. Salamo, B. Crosignani, and P. DiPorto, *Elect. Lett.* **31**, 826 (1995).
9. M. Shih, M. Segev, G. C. Valley, G. Salamo, B. Crosignani, and P. DiPorto, *Opt. Lett.* **21**, 324 (1996).
10. K. Kos, H. Ming, G. Salamo, M. Shih, M. Segev, and G. C. Valley, *Phys. Rev. E* **53**, R4330 (1996).
11. M. Shih, Z. Chen, M. Mitchell, M. Segev, H. Lee, R. Feigelson, and J. Wilde, *J. Opt. Soc. B* **14**, 3091 (1997).
12. S. Lan, E. DelRe, Z. Chen, M. Shih, and M. Segev, *Opt. Lett.* **24**, 475 (1999).
13. M. Taya, M. C. Bashaw, M. M. Fejer, M. Segev, and G. C. Valley, *Opt. Lett.* **21**, 943 (1996).
14. Z. Chen, M. Mitchell, and M. Segev, *Opt. Lett.* **21**, 716 (1996).
15. J. Pette and C. Denz, *Opt. Commun.* **188**, 53 (2001).
16. B. Luther-Davies and X. Yang, *Opt. Lett.* **17**, 496 (1992).
17. S. Lan, M. Shih, G. Mizell, J. A. Giordmaine, Z. Chen, C. Anastassiou, and M. Segev, *Opt. Lett.* **24**, 1145 (1999).
18. S. Lan, M. Shih, G. Mizell, J. A. Giordmaine, Z. Chen, C. Anastassiou, and M. Segev, *Appl. Phys. Lett.* **77**, 2101 (2000).
19. M. Klotz, H. Meng, M. Segev, and S. R. Montgomery, *Opt. Lett.* **24**, 77 (1999).
20. E. DelRe, M. Tamburrini, M. Segev, A. Agranat, and R. Della Pergola, *Phys. Rev. Lett.* **83**, 1954 (1999).